# Interaction of *Vitreoscilla* Hemoglobin with Membrane Lipids†

Andrea C. Rinaldi,‡ Alessandra Bonamore,§ Alberto Macone,§ Alberto Boffi,*,§ Argante Bozzi,|| and Antonio Di Giulio||

*Dipartimento di Scienze e Tecnologie Biomediche, Sezione di Chimica Biologica e Biotecnologie Biochimiche, Università di Cagliari, I-09042 Monserrato (CA), Italy, Dipartimento di Scienze Biochimiche, Università "La Sapienza", I-00185 Roma, Italy, and Dipartimento di Scienze e Tecnologie Biomediche, Università dell'Aquila, Via Vetoio, I-67100 L'Aquila, Italy*

*Received November 7, 2005; Revised Manuscript Received January 30, 2006*

ABSTRACT: The interaction of the recombinant hemoglobin from *Vitreoscilla* sp. (VHb) with the bacterial membrane of *Escherichia coli* cells has been investigated by measuring the propensity of VHb to interact with monolayers formed by natural bacterial phosholipids. The measurements showed that the protein is capable of penetrating the monolayers, possibly establishing interactions with the hydrophobic acyl chains. VHb is also capable of binding reversibly phospholipids and free fatty acids in solution with a strong selectivity toward cyclopropanated acyl chain species. Lipid binding occurs within the distal heme pocket as demonstrated by a sharp UV−vis spectral change corresponding to a five-coordinate to six-coordinate transition of the heme−iron ferric derivative. Oxygen binding properties are affected by the presence of the lipid component within the active site. In particular, the oxygen affinity is decreased by more than 20-fold in the presence of cyclopropanated phospholipids. The kinetic counterpart of the decrease in oxygen affinity is manifest in a 10-fold decrease in the ligand combination kinetics. Accordingly, the CO and NO combination kinetics were also significantly affected by the presence of the bound lipid within the active site. These studies indicate that the current functional hypotheses about VHb should take into account the association of the protein within the cytoplasmic membrane as well as the presence of a phospholipid within the active site. These data suggest a possible lipid-induced regulation of oxygen affinity as the basis of VHb functioning.

The bacterial hemoglobin from *Vitreoscilla* species (VHb)[1] represents a most versatile tool for a variety of whole cell biotechnological processes (*1*). In fact, heterologous expression of VHb within bacteria, yeasts, fungi, and plant cells has been successfully exploited to enhance host cell growth (*2*) and to improve the expression of selected enzymes (*3*) or the yield of valuable intermediate metabolites (*4*), especially under oxygen-limiting conditions. Notable examples of the in vivo effects of VHb include the increased production of α-amylase in *Escherichia coli* (*5*) and cephalosporin C in *Acremonium chrysogenum* (*6*), the degradation of toxic wastes such as benzoic acid by *Pseudomonas* species and 2,4-dinitrotoluene by *Burkholderia* (*7*), and the enhanced activity of chimeric VHb-amino acid oxidases (*8*, *9*).

Such an amazingly wide array of biotechnological applications of VHb contrasts with a poorly understood biochemical reactivity toward heme ligands and uncertain physiological role(s). Increased levels of tRNAs and ribosomes as well as enhanced respiratory activity and ATP production have been reported as major beneficial consequences of VHb expression in heterologous hosts (*10*, *11*). However, the explicit mechanism that links the overall metabolic effects to the putative "hemoglobin-like" function of VHb is as yet unclear. At present, the following two general hypotheses have been put forth: (i) VHb acting as a scavenger toward oxygen or NO radicalic species (*12*) or (ii) VHb acting as an oxygen delivering protein (myoglobin-like) that facilitates the oxygen diffusion toward terminal oxidases (*13*, *14*). The latter hypothesis implies that the presence of VHb within the respiratory membrane enhances the oxygen flux to one or both terminal oxidases (cytochromes *bo* and *bd* in *E. coli*) under hypoxic conditions. The observation that exogenously added VHb stimulated the ubiquinol oxidase activity of both the respiratory membrane and the cytochrome *bo* proteoliposomes provided evidence that the interaction between VHb and cytochrome *bo* is physiologically important (*14*).

Therefore, the interaction of VHb with the phospholipid membrane of the heterologous host (*E. coli*) appears to play a pivotal role and requires further investigation especially in light of previous observations about the similar flavohemoglobin from *E. coli* (HMP). In fact, both VHb and HMP have been reported to partition efficiently to the phospholipid bilayer (*13*, *15*), and the latter protein has been also demonstrated to bind phospholipids within the active site.

† Research Projects COFIN 2004 to A. Boffi and A. Bozzi and FIRB 2003 to A. Boffi from MIUR (Ministero dell'Università e della Ricerca) are gratefully acknowledged. This work is partially supported by Istituto Pasteur, Fondazione Cenci Bolognetti, to A. Boffi.

* To whom correspondence should be addressed: Dipartimento di Scienze Biochimiche, Università "La Sapienza", P. Aldo Moro 5, 00185 Rome, Italy. Phone: +39 06 4991 0990. Fax: +39 06 4440 062. E-mail: alberto.boffi@uniroma1.it.

‡ Università di Cagliari.

§ Università "La Sapienza".

|| Università dell'Aquila.

[1] Abbreviations: VHb, *Vitreoscilla* hemoglobin; HMP, *E. coli* flavohemoglobin; FHP, *Alcaligenes eutrophus* (*Ralstonia eutropha*) flavohemoglobin; TLE, total lipid extracts from *E. coli* membranes; UFA, unsaturated fatty acids.

10.1021/bi052277n CCC: $33.50 
Published on Web 03/11/2006

The lipid binding properties, together with alkylhydroperoxide reductase activity, suggested a specific role for HMP in the bacterial response to oxidative/nitrosative stress. The structural similarity of VHb and HMP is restricted to the first shell of residues that form the contour the heme pocket (*16*−*18*), whereas notable differences between the two proteins are evident in the neighboring regions, especially within the solvent-exposed CE segment that limits the external surface of the active site. Nevertheless, the hydrophobic nature of the distal site and the conservation of the distal LeuE11, PheB9, and TyrB10 triad suggest that the two proteins may display a common behavior with respect to lipid binding properties, protein−membrane interaction, and oxygen binding properties.

In this work, the interaction of VHb with *E. coli* membranes has been addressed by means of lateral pressure measurements on monomolecular phospholipid films. This system has become increasingly popular as a model for investigating the interactions of a wide range of proteins and peptides with biological membranes (*19*−*21*) in that it can confirm directly and with high sensitivity the protein−monolayer interaction. Moreover, VHb was also demonstrated to bind reversibly cyclopropanated phospholipids (and fatty acids) within the active site with consequent alteration of the oxygen binding properties.

## MATERIALS AND METHODS

Recombinant *Vitreoscilla* Hb was expressed in *E. coli* BL21 cells and purified as described previously (*22*). To ensure complete removal of bound phospholipids, an additional purification step on the lipid avid hydroxylalkoxypropyldextran resin (Type X, Sigma-Aldrich Co.) was carried out. Phospholipids and cyclopropanehexadecanoic, -linoleic, -oleic, and -*cis*-vaccenic acids were obtained from Larodan Fine Chemicals (Malmö, Sweden).

Total lipid extracts (TLE) from *E. coli* BL21 cells were prepared as described previously (*15*). Fatty acid methyl esters were analyzed by gas chromatography−mass spectrometry (GC−MS) using an Agilent 6850A gas chromatograph coupled to a 5973N quadrupole mass selective detector (Agilent Technologies, Palo Alto, CA). Chromatographic separations were carried out on a Zebron ZB-WAX fused-silica capillary column (30 m × 0.25 mm inside diameter) coated with polyethylene glycol (film thickness of 0.25 $\mu$m) as stationary phase. The injection mode was splitless at 260 °C. The column temperature program was from 150 °C (1 min) to 260 °C at a rate of 5 °C/min and held for 20 min. The carrier gas was helium at a constant flow of 1.0 mL/min. The spectra were obtained in the electron impact mode with an ionization energy of 70 eV and a mass range scan from *m*/*z* 50 to 500, an ion source temperature of 280 °C, and an ion source vacuum of $10^{-5}$ Torr.

*Monolayer Experiments.* Insertion of *Vitreoscilla* Hb into monolayers of plasma membrane lipids extracted from *E. coli* (TLE) and spread at an air−buffer (10 mM sodium phosphate at pH 7.2) interface was monitored by measuring the surface pressure ($\pi$) with a Wilhelmy wire attached to a microbalance (DeltaPi, Kibron Inc., Helsinki, Finland) connected to a personal computer and using circular glass wells (subphase volume of 0.5 mL). After evaporation of lipid solvent (2:1 chloroform/methanol mixture) and stabilization of monolayers at different initial surface pressures ($\pi_0$), the protein (0.05−1.5 $\mu$M) was injected into the subphase, and the increment in surface pressure of the lipid film upon intercalation of the protein dissolved in the subphase was followed for the next 37 min. The difference between the initial surface pressure and the value observed after the penetration of *Vitreoscilla* Hb into the film was taken to be $\Delta\pi$. Data shown in Figure 1 represent the last set of five independent measurements carried out on different protein and phospholipid preparations, all showing good reproducibility. All measurements were performed at room temperature.

*Lipid Binding Measurements.* Phospholipid and free fatty acid binding properties were measured essentially as described in ref *15*. Briefly, the lipid-free VHb solution [8 $\mu$M, in 0.1 M phosphate buffer (pH 7.0) containing 20% (v/v) ethanol] in the ferric state was titrated with small amounts of ethanolic solutions containing either TLE or free fatty acids. Phospholipid and fatty acid concentrations in ethanol were standardized by infrared absorption measurements in the carbonyl stretching region (1690−1720 $cm^{-1}$) as described in ref *15*. The UV−vis spectra were recorded between 250 and 700 nm on a Jasco V-570 spectrophotometer (Jasco Ltd.). Kinetic experiments were carried out by means of stopped-flow measurements in an Applied Photophysics (Leatherhead, U.K.) instrument. Phospholipid binding was also monitored by GC−MS (on methyl ester extracts) and UV−vis spectroscopy on protein samples collected after each step of the purification procedure. Thus, a ferric protein sample was examined by UV−vis spectroscopy and then extracted with a chloroform/methanol mixture (see the previous paragraph) at each purification stage (*22*), namely, after the capture (DEAE52 anion exchange chromatography), enrichment (hydroxylapatite chromatography), and refinement (G-75 Sephadex gel filtration chromatography) steps.

*Oxygen Binding Properties.* The oxygen binding kinetics was measured by directly mixing the deoxygenated protein with buffer containing varying amounts of dissolved oxygen. In this case, the deoxygenated protein solution was prepared according to the method of Kundu et al. (*23*). The reduced protein (8 mL total volume, 5 $\mu$M heme) was transferred to a gastight stopped-flow syringe, and 2 mL of a 5 mg/mL G6P dehydrogenase solution was added. The syringe was kept for 15 min in the stopped-flow apparatus until the signal at 430 nm (the peak of the deoxygenated derivative) reached a stable value indicating that the protein was fully deoxygenated. Thereafter, the deoxygenated protein was mixed with oxygenated buffer containing varying amounts of oxygen (135, 65, 32.5, and 16 $\mu$M before mixing).

Oxygen release kinetics were also measured in an oxygen pulse experiment by mixing a solution of either lipid-bound (TLE) or lipid-free VHb (8 $\mu$M) containing an excess of sodium dithionite (0.2−20 mM) in 0.25 M phosphate buffer at pH 7.0 with oxygenated buffer. At each dithionite concentration, time courses were collected over 10 s by following the absorbance decrease at 430 nm and the corresponding increase at 416 nm. Thereafter, the oxygen pulse experiment was carried out as a function of oxygen concentration by diluting the oxygenated buffer with a degassed one. Four oxygen concentrations were examined: 135, 65, 32.5, and 16 $\mu$M (before mixing).

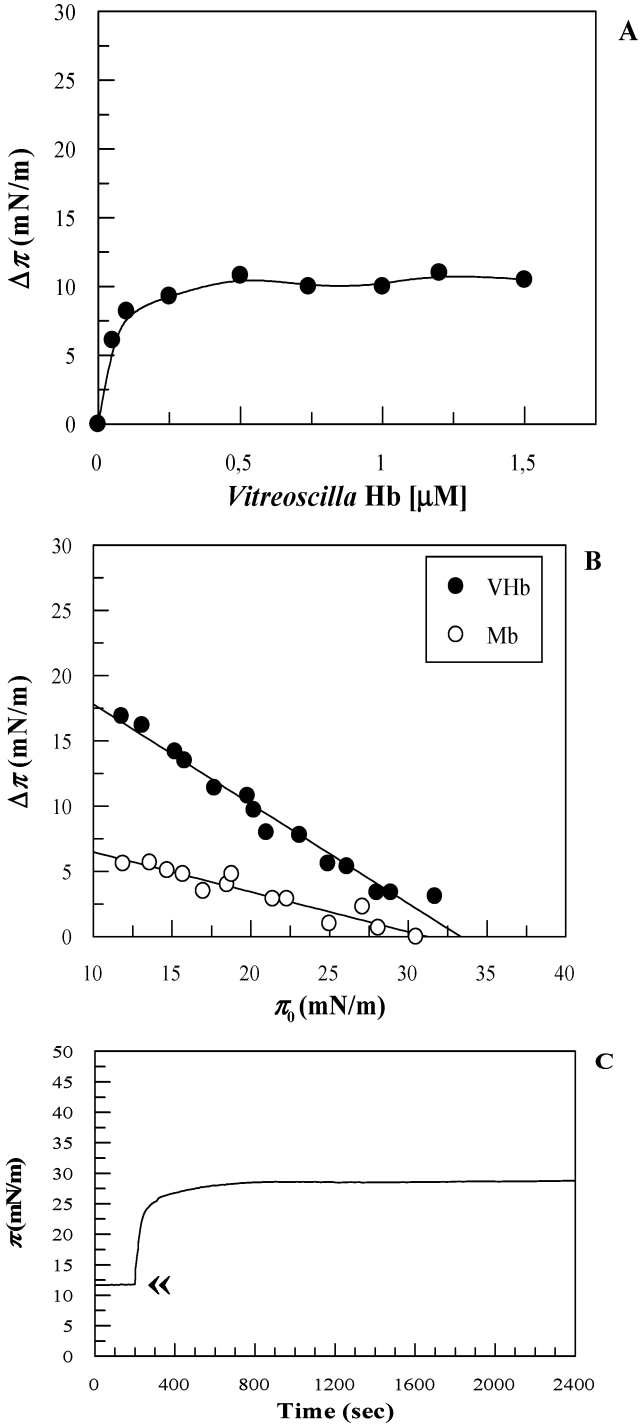


FIGURE 1: Insertion of *Vitreoscilla* Hb into *E. coli* lipid monolayers. Increments of surface pressure of *E. coli* lipid monolayers due to the addition of *Vitreoscilla* Hb into the subphase are illustrated as a function of protein concentration (A, at an initial surface pressure varying between 19.8 and 20.2 mN/m) or initial surface pressure [B, with 0.5 $\mu$M protein; horse Mb controls (○)]. Typical kinetics of surface pressure increase related to penetration of *Vitreoscilla* Hb into *E. coli* lipid monolayers (C, $\pi_0 = 11.8$, with 0.5 $\mu$M protein; arrow indicates injection of the protein into the subphase).

*CO and NO Binding Properties.* CO combination kinetics were studied in stopped-flow experiments by mixing either lipid-free or lipid-bound dithionite (20 mM)-reduced VHb with CO-containing solutions in 0.2 M phosphate buffer at pH 7.0 and in the presence of 20 mM dithionite at 20 °C. Under the same experimental conditions, binding of NO to ferrous VHb could not be monitored as the reaction occurred within the dead time of the instrument even at low NO concentrations and 5 °C. Thus, NO binding kinetics were measured on the ferric VHb derivatives by directly mixing anaerobic NO solutions with the ferric, lipid-bound, or lipid-free protein. Anaerobic NO-saturated solutions were prepared by bubbling NO gas at 1 atm through a NaOH trap and equilibrating the degassed buffer with NO gas in a tonometer. Reactions were monitored at 419 nm (the peak of the ferric NO derivative) or 404 nm (the absorption maximum of the ferric protein). CO release kinetics were measured in a diode array spectrophotometer by adding an increasing amount of anaerobic NO-containing buffers to the CO-saturated protein. The protein concentration was 4 $\mu$M, and the CO concentration was 10 $\mu$M.

## RESULTS

*Interaction of Vitreoscilla Hb with the E. coli Lipid Monolayer.* Addition of a ferric *Vitreoscilla* Hb solution to the liquid phase underlying *E. coli* lipid monolayers caused a sudden increase in the film surface pressure (Figure 1). Under the experimental conditions detailed in Materials and Methods, the $\Delta\pi$ shift was dependent on protein concentration, reaching a plateau around 0.5 $\mu$M *Vitreoscilla* Hb (Figure 1A), which was therefore selected as the optimal protein concentration for subsequent experiments. When data from similar measurements were analyzed in terms of $\Delta\pi$ versus $\pi_0$, the critical surface pressure corresponding to the lipid lateral packing density preventing the intercalation of the protein into *E. coli* lipid films could be derived by extrapolating the $\Delta\pi-\pi_0$ slope to a $\Delta\pi$ of 0, giving a value of ≈33 mN/m (Figure 1B). The kinetics of the insertion of the protein into the lipid monolayer were characterized by a rapid and marked increase in surface pressure that followed injection of the protein into the subphase, the lag phase for this process being too short to be measurable with our instrumentation (Figure 1C). In a typical experiment, within 120 s of protein injection, $\pi$ attained slightly more than 90% of that recorded at the end of the measurement (Figure 1C). This initial peak was then followed by a slow increase in $\pi$ for approximately the next 8 min, when a plateau was reached, and no more variation in $\pi$ was detected up to 30 min. This kinetic pattern was independent of initial surface pressure and, to a lesser extent, protein concentration, because when low (0.05−0.25 $\mu$M) *Vitreoscilla* Hb concentrations were used the initial spike in the increase of surface pressure was strongly diminished or negligible (not shown). As a whole, the data demonstrate that VHb efficiently penetrates the phospholipid monolayer. Control experiments demonstrated that the interaction of horse myoglobin with the membrane monolayer does occur, but to a much lesser extent with respect to VHb (Figure 1B) and with a very slow kinetics (data not shown). The data for horse myoglobin are consistent with earlier reports (*13*) and point to a nonspecific interaction of the protein with biological membranes.

*Lipid Binding Properties in Solution.* The presence of a bound phosholipid within the VHb active site was initially suspected on the basis of the UV−visible spectral changes observed for the ferric protein during the purification procedure. Ferric protein samples were thus examined by UV−vis spectroscopy and then extracted and esterified with an acidic chloroform/methanol mixture at each purification stage. The analysis of the GC−MS profiles of methyl ester

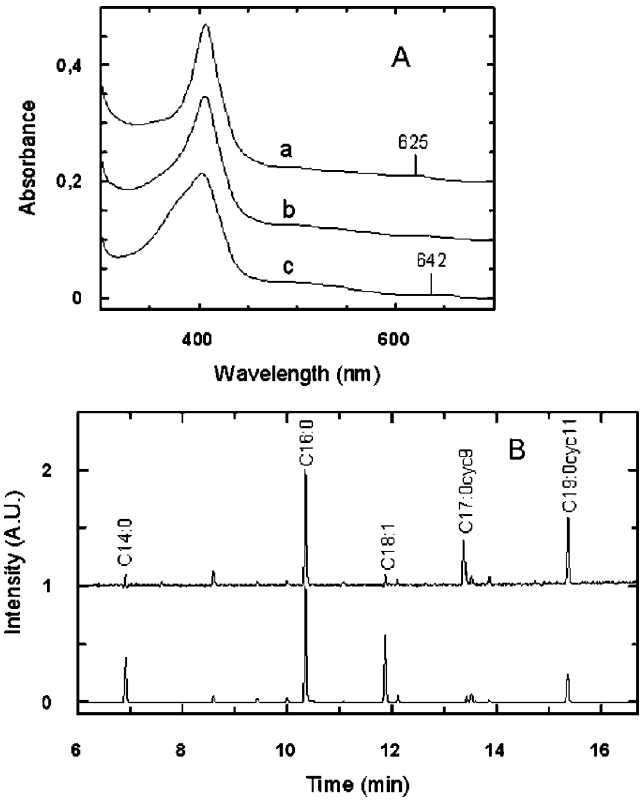


FIGURE 2: UV−vis spectra of *Vitreoscilla* Hb at different purification steps and GC−MS FAME profile of the phospholipids extracted from the partially purified protein. The visible spectra in panel A refer to the samples of ferric VHb as obtained after the purification steps with (a) DEAE52 (first step), (b) hydroxylapatite (second step), and (c) G-75 Sephadex (third step) chromatographies. The transition from a six-coordinated high-spin heme iron to a five-coordinate high-spin derivative is evident in passing from spectrum a to c. In the GC−MS FAME profiles shown in panel B, the total lipid extracts from the *E. coli* bacterial membrane fraction (bottom profile) are compared to the fatty acid methyl esters obtained from phospholipids extracted from VHb after the anion exchange chromatographic step (top profile).

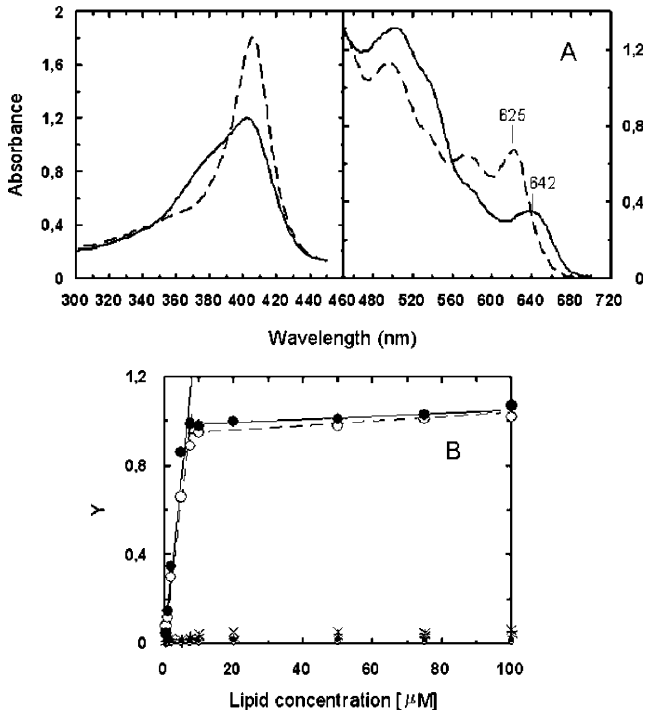


FIGURE 3: UV−vis spectra of ferric phospholipid-bound vs phospholipid-free *Vitreoscilla* Hb and phosholipid titration experiments. Spectra in panel A were measured on a 12.5 $\mu$M (heme) ferric protein solution in 0.1 M phosphate buffer at pH 7.0 and 20 °C before (—) and after (− − −) addition of a 10-fold molar excess of total *E. coli* phospholipids (dissolved in a 3:1 ethanol/chloroform mixture, 15 $\mu$L over a total volume of 3.5 mL). The fractional saturation (*Y*) was calculated from wavelength-averaged absorbance differences and was plotted as a function of lipid concentration in panel B. Titrations were carried out in a 8 $\mu$M protein solution in phosphate buffer at pH 8.0 by adding small amounts of ethanolic lipid solutions. Lipid species were (○) TLE, (×) dipalmitoylphosphatidylethanolamine, (•) dipalmitoylphosphatidylethanolamine, (∗) linoleic acid, (◦) oleic acid, (+) palmitoleic acid, and (●) cyclopropanepalmitoleic acid.

extracts from partially purified VHb after the capture and enrichment steps revealed that only phospholipids containing cyclopropanated fatty acids copurified with VHb (Figure 2). A trace amount of bound phospholipids was detected even after the refinement step and could be removed by lipid affinity chromatography to ensure the preparation of homogeneous lipid-free protein samples. The bound phospholipid has been identified by GC−MS as a phosphatidylglycerol esterified with a saturated C16 fatty acid in the *sn*-1 position and a C17:0,cyc9 or a C19:0,cyc11 cyclopropanated fatty acid in the *sn*-2 position (Figure 2). It should be mentioned that cyclopropanated fatty acids represent the major fatty acid component of the lipid membrane in *E. coli* during the stationary phase.

On the basis of the spectral assignments in Figure 3A, the spectral changes shown in Figure 2 were assigned to the progressive loss of the iron-bound phospholipid component along the purification procedure. In particular, the line shape of the Soret band is broadened after phospholipid removal and the ferric heme iron charge transfer peak shifts from 625 nm in the lipid-bound protein (after the first purification step) to 642 nm in the lipid-free protein. As previously demonstrated for HMP, the observed spectral changes correspond to a typical pentacoordinated to hexacoordinated ferric high-spin heme transition and indicate that a direct interaction of a lipid component with the ferric heme iron must occur (*15*).

Subsequent titration of lipid-free VHb with TLE or free fatty acids (Figure 3B) revealed that the protein recognizes exclusively cyclopropanated fatty acids (C17:0,cyc9 or C19:0,cyc11) both as free acids and as phospholipid components, whereas no lipid-induced spectral signals were observed in the case of UFAs (oleic or linoleic) or phospholipids containing saturated (dipalmitoylphosphatidylethanolamine) or unsaturated fatty acids (dipalmitoleylphosphatidylethanolamine). Thus, VHb exhibits a narrow specificity toward the nature of the phospholipid fatty acid acyl chains at least with respect to HMP [that appeared to possess the highest affinity for linoleic acid (*15*)].

*Oxygen Binding Properties.* Oxygen binding properties of VHb have been determined in kinetic experiments of oxygen combination and release. Oxygen combination measurements had been previously carried out on fully purified VHb by means of a laser photolysis technique (*22*). These measurements allowed estimation of a very fast second-order rate for oxygen binding, characterized by a combination constant of $\sim 2 \times 10^8$ $M^{-1}$ $s^{-1}$. The same experiment, carried out on the oxygenated, lipid-bound (TLE or C17:0,cyc9) VHb, gave unclear results due to a very low yield of photolysis (<0.1%,

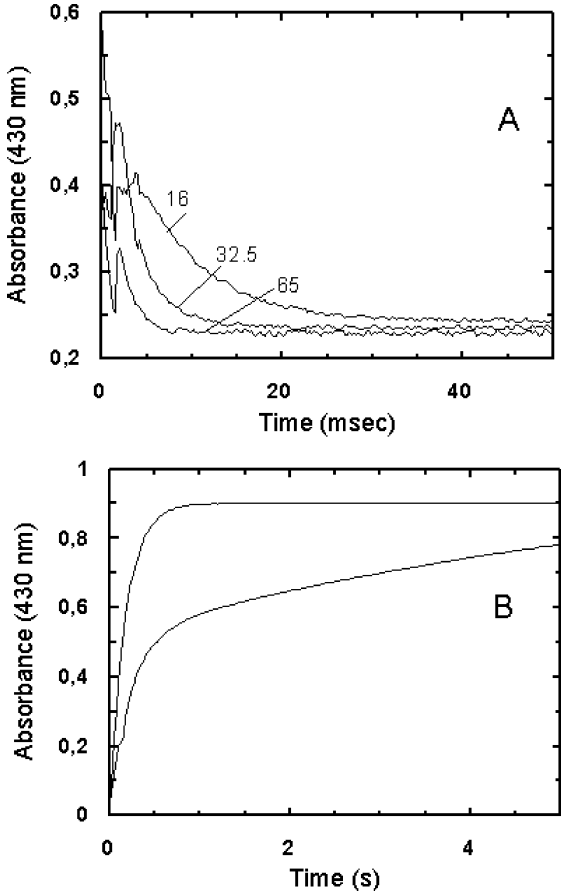


FIGURE 4: Kinetics of oxygen binding and release in lipid-bound *Vitreoscilla* Hb. Time courses for binding of oxygen to VHb complexed with TLE are shown in panel A at different oxygen concentrations. Rapid mixing experiments were carried out at 20 °C in 0.1 M phosphate buffer at pH 7.0 by mixing deoxygenated VHb in the presence of an enzymatic system for oxygen consumption (see Materials and Methods) with oxygen-containing buffers. The signal decay at 430 nm corresponds to the disappearance of the deoxygenated species. The first 4−5 ms in the kinetic records corresponds to the dead time of the instrument. Oxygen release kinetics measured in oxygen pulse experiments are shown in panel B. The bottom curve was obtained with lipid-free protein, and the top curve depicts data from the release of oxygen from the lipid-bound species.

data not shown) and a relatively fast autoxidation rate. However, it was observed that the oxygen combination rate was greatly reduced with respect to that of the lipid-free protein. Therefore, direct stopped-flow experiments were carried out by mixing deoxy-VHb (enzymatically reduced) with oxygen-containing buffers at both 5 and 20 °C. The kinetic records of Figure 4A show that oxygen binding can be fully analyzed in terms of pseudo-first-order conditions despite the poor signal recovery in the first 4−5 ms after mixing at the highest oxygen concentration used, at 20 °C. Control experiments were also carried out at 5 °C to assess the total signal recovery (total Δ absorbance deoxy minus oxy at 430 nm) under these conditions. The second-order oxygen binding constant thus obtained was $(8.8 \pm 1.6) \times 10^6$ $M^{-1}$ $s^{-1}$ at 20 °C (see Table 1). Oxygen release data, as measured by the oxygen pulse experiments, yielded time courses that were independent of oxygen concentration at a dithionite concentration of >10 mM and yielded a first-order rate of 6.6 $s^{-1}$.

Table 1: Kinetic Parameters[a] of Binding of Oxygen to and Release of Oxygen from *Vitreoscilla* Hb

| | $k_{on}$ ($\mu M^{-1}$ $s^{-1}$) | $k_{off}$ ($s^{-1}$) | $K$ ($\mu M^{-1}$) | ref |
|---|---|---|---|---|
| lipid-free ($O_2$) | 200 | 4.2 | 47.6 | *22* |
| | | 0.15 | 1330 | *22* |
| lipid-bound ($O_2$) | 8.8 | 6.6 | 1.30 | this work |
| lipid-free (CO) | 7.5 | 0.0036 | 208 | this work |
| lipid-bound (CO) | 0.58 | 0.011 | 52 | this work |
| lipid-free (NO)[b] | 8.4 | − | − | this work |
| lipid-bound (NO)[b] | 0.35 | − | − | this work |

[a] Measurements were carried out in 0.1 M phosphate buffer at pH 7.0 and 20 °C. [b] The NO binding kinetics refer to the ligand binding to the ferric derivative.

*CO and NO Binding Kinetics.* The CO combination kinetics, measured either on the lipid-bound or lipid-free protein, were strongly biphasic. In particular, in lipid-free VHb, a pseudo-first-order fast phase was followed by a slower contribution showing an anomalous CO concentration dependence. The amplitude of the fast phase was dominating (>90%) at CO concentration of <100 $\mu$M but increased up to 30−35% at 250 $\mu$M CO. The pseudo-first-order graph of Figure 5 was obtained by plotting the fast phases only as a function of CO concentration. In the lipid-saturated protein, the slow contribution to the kinetics of CO binding was greatly reduced (<8%). CO release kinetics in the presence and absence of the bound lipid were also measured by NO displacement experiments. The lipid-bound protein was capable of a faster CO release (0.011 $s^{-1}$) with respect to the lipid-free protein (0.0036 $s^{-1}$). The kinetics of NO binding to the ferric lipid-bound or lipid-free protein were also measured by stopped-flow experiments. As in the case of CO binding to the ferrous protein, the kinetics were biphasic in the lipid-free protein and essentially monophasic in the lipid-bound derivative. The UV−vis absorption spectra of the NO-bound ferrous and ferric VHb were not reported previously and are shown in Figure 6. It is of interest to consider that the ferric NO complex is fairly stable in VHb, although it undergoes a slow reduction process over a time scale of several hours (data not shown).

## DISCUSSION

The main target of this work was to single out and correlate the lipid−membrane interaction and the oxygen binding properties of VHb to establish whether these properties may be physiologically relevant.

The interaction of VHb with the *E. coli* membrane has been addressed by measurements of lateral pressure in phospholipid monolayers obtained from total *E. coli* lipid extracts. The pressure shift induced by addition of VHb, with respect to horse Mb controls, provides striking evidence of an unexpectedly strong and kinetically fast interaction of the protein with the monolayer. Indeed, the observed $\Delta\pi$ demostrates that VHb physically penetrates the monolayer, intercalating between the lipid molecules spread at the air−water interface (*8*). As previously recognized (*13*, *14*), VHb is devoid of any known membrane insertion motif or periplasmic export peptides at the N-terminal sequence. Thus, the rationale for the observed effects must reside in a major conformational transition that allows for an energetically favorable contact of hydrophobic residues of the protein with the hydrocarbon moiety of the phospholipids, although the

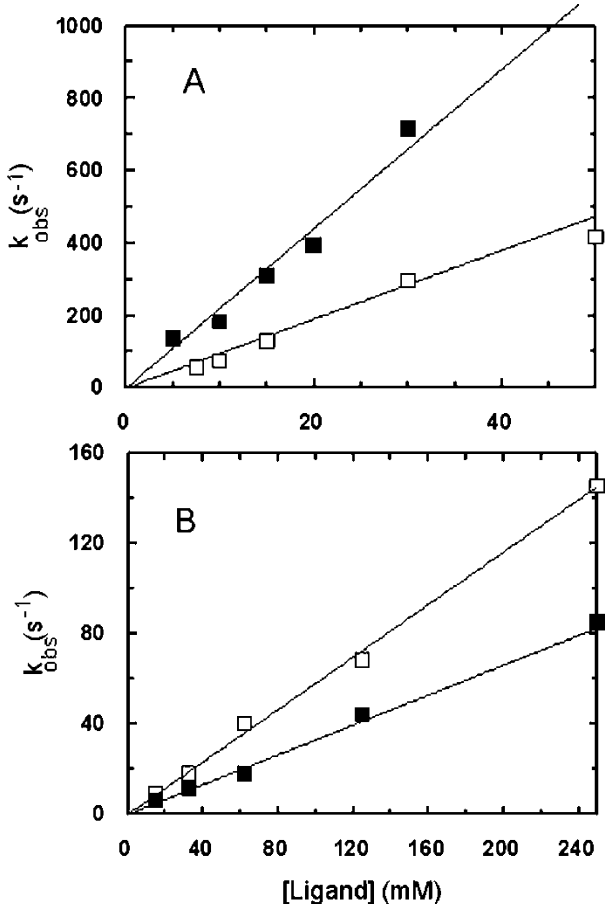


FIGURE 5: Pseudo-first-order plots for binding of CO and NO to ferrous and ferric *Vitreoscilla* Hb, respectively. CO combination kinetics with the ferrous VHb derivative (□) and NO binding kinetics with the ferric protein (■) were measured in lipid-free (A) and lipid-bound (B) VHb derivatives. Reactions were monitored in stopped-flow experiments by mixing either lipid-free or lipid-bound dithionite (20 mM), reduced VHb with CO-containing solutions in 0.2 M phosphate buffer at pH 7.0 and in the presence of 20 mM dithionite at 20 °C. NO binding kinetics were measured on the ferric VHb derivatives by directly mixing an anaerobic NO solution with the ferric, lipid-bound or lipid-free protein in 0.2 M phosphate buffer at pH 7.0 and 20 °C. Reactions were monitored at 419 nm (the peak of the ferric NO derivative) or 404 nm (the absorption maximum of the ferric protein).

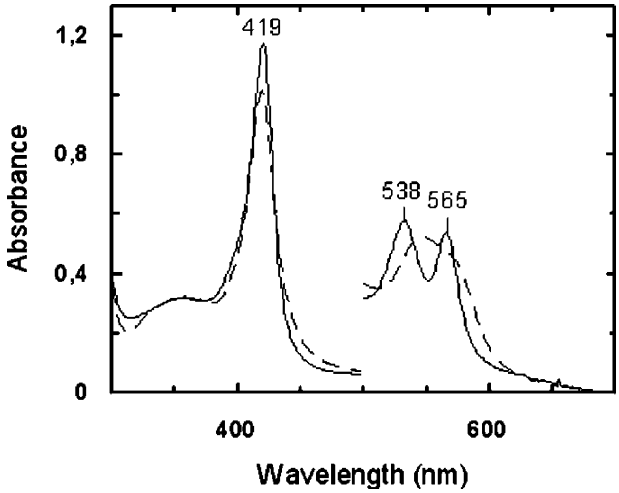


FIGURE 6: UV−visible spectra of ferrous and ferric *Vitreoscilla* Hb−NO adducts. The spectra are for the NO-bound ferric (—) and ferrous (− − −) VHb derivative. The protein concentration was 7.5 $\mu$M in 0.2 M phosphate buffer at pH 7.0 under 1 atm of $N_2$ gas. The reduced NO derivative was obtained by adding a 10-fold molar excess of dithionite to the ferric NO adduct. The spectra were indentical both in the presence and in the absence of the bound phospholipid molecule.

possibility that ionic interactions between the charged and polar residues of the protein and the polar phospholipid head might also take place cannot be excluded, most likely favoring the initial protein binding at the monolayer surface. At present, such a conformational transition can only be inferred to occur through the participation of amphipathic α-helices that line the heme pocket with consequent exposure of the highly hydrophobic distal pocket to the acyl chain moiety. In particular, it may be envisaged that the flexible region between the CE corner and the E helix (comprising residues on the top of the heme pocket; see Figure 7) serves as a phospholipid anchoring device, thus allowing for a direct interaction of the heme moiety with the lipid acyl chain. Along this line, when the structures of lipid-free HMP and lipid-bound FHP are compared, the CE region (not visible in VHb) appears as a lid that closes when the phospholipid enters the heme pocket, a picture that is reminiscent of the lipid binding module in some lipases (*24*).

These hypotheses served as a starting point for analyzing whether the soluble VHb fraction obtained after bacterial lysis contained a phospholipid bound within the active site, as reported earlier for *Alcaligenes eutrophus* and *E. coli* flavohemoglobins (*15*, *25*, *26*). Both UV−vis spectroscopy and GC−MS analysis demonstrated unambiguously that VHb is fully saturated with a phosphatidylglycerol esterified with a saturated C16 fatty acid in the *sn*-1 position and a C17:0,cyc9 or a C19:0,cyc11 cyclopropanated fatty acid in the *sn*-2 position. The sharp UV−vis transition that accompanies lipid binding can almost be superimposed with that observed in HMP and correponds to a five-coordinate to six-coordinate high-spin transition of the ferric heme, thus implying the presence of a bonding interaction between the heme iron and a phospholipid/fatty acid component. As in HMP, no spectral signal could be detected upon binding of lipid to the ferrous species (*15*, *27*). The nature of the bond between the ferric iron and the lipid chain is as yet unclear. In the case of the HMP−linoleic acid complex, it was proposed that bonding could result from a $\pi$-type interaction between the iron $d_{z^2}$ orbital and the $\pi$ system of linoleic acid (*27*). In VHb, however, no spectral transition could be observed in the presence of linoleic acid in that only cyclopropanated species are able to generate the spectral changes reported in Figure 2. The mode of binding of the cyclopropanated phospholipid (or fatty acid) most likely reflects that observed by Ollesch et al. (*26*) in the case of FHP, in which the cyclopropyl moiety of the phospholipid resides 3.6 Å from the metal in the ferrous derivative. On this basis, a possible hypothesis is that the iron $d_{z^2}$ orbital (in the ferric state) is capable of overlapping with the strained C−C $\sigma$ orbital of the cyclopropyl ring. If confirmed, this interaction would represent the first example of a direct ferric iron−saturated hydrocarbon bonding interaction.

The presence of a lipid acyl chain within the distal pocket of the heme implies that the heme ligand binding properties must be re-evaluated by taking into account the occupancy of the lipid component within the distal site. Oxygen binding and dissociation data obtained for lipid-bound versus lipid-free VHb reveal several intriguing features. First, it is of

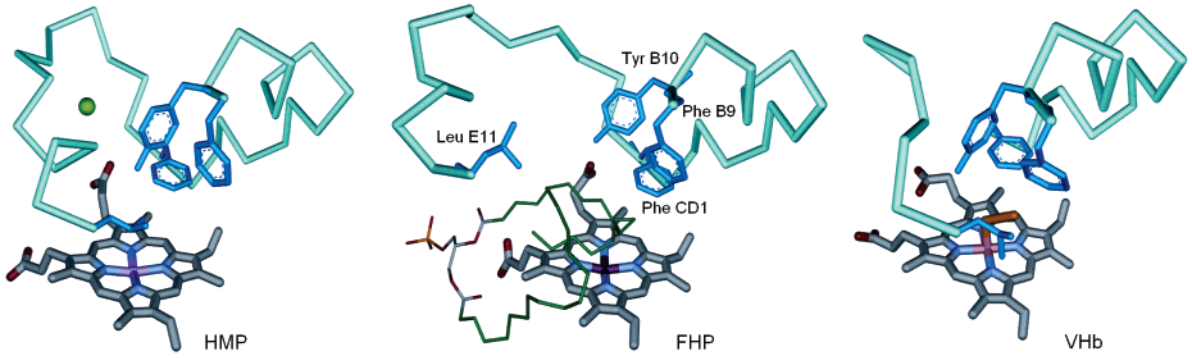


FIGURE 7: Close-up of the active sites of *Vitreoscilla* hemoglobin, *A. eutrophus* and *E. coli* flavohemoglobins. The crystal structures of the distal heme pockets of azido-met VHb (PDB entry 2VHB), ferrous lipid-bound *A. eutrophus* FHP (PDB entry 1CQX), and ferric unliganded HMP (PDB entry 1GVH) are compared. The regions corresponding to the B helix, the CE corner, and the beginning of the E helix are shown as pale blue tubes. Part of the CE loop is a disordered segment in VHb and is not shown. The chloride ion in the CE loop region of HMP is represented as a green sphere. The phospholipid acyl chains in FHP are colored green, and conserved distal residues in the three proteins are colored cyan. The iron-bound azide in VHb is colored brown.

interest to note that the kinetics of oxygen binding and release to VHb are perfectly monophasic in the presence of bound phospholipids, whereas a strongly biphasic behavior was observed in the lipid-free protein (*22*). Second, the overall oxygen affinity, as estimated from the ratio between the kinetic constants, is greatly decreased (>20-fold) in the presence of the phospholipid component. It is worth noting that the figure obtained for the second-order combination constant in lipid-bound VHb ($8.8 \times 10^6$ $M^{-1}$ $s^{-1}$) falls within the range of previous laser photolysis measurement carried out on native VHb (*28*) which was considered in open discrepancy with our former measurements carried out on the lipid-free protein (*22*). The marked effect on the oxygen binding kinetics prompted a parallel study of the ligand binding properties with other biatomic ligands, namely, CO (with the ferrous reduced protein) and NO (with the ferric VHb derivative). The results obtained (see Table 1) fully confirmed the strong decrease in the second-order combination constants together with a slight increase in the rate of ligand release, in the CO dissociation reaction. On the basis of these results, it is important to mention that there is no apparent rate-limiting step in the ligand combination reactions of CO with the ferrous protein and of NO with the ferric VHb derivative. Thus, especially in the ferric derivative, the dissociation of the iron−lipid coordination bond (a prerequisite for NO binding) must be extremely fast, and a lipid acyl chain rotameric rearrangement within the heme pocket most likely accounts for it rather the release of the phospholipid molecule to the solvent. On this basis, it may be envisaged that ligand binding and release to the heme iron in the lipid-saturated protein may occur while the acyl chain still resides within the distal pocket and eventually contributes to the formation of a distal shell in contact with the bound ligand. X-ray structural data on the iron-liganded, lipid-bound protein derivative will be necessary to clarify this point.

In light of these results and of the previous similar data obtained for HMP (*15*), it should be stressed that the contribution of lipid to binding of gaseous ligand to bacterial hemoglobins (either single-chain proteins or flavohemoglobins) cannot be overlooked. Along this line, the recently reported differences among ligand binding properties in a number of single-chain hemoglobins and flavohemoglobins might be re-evaluated on the basis of the possible presence or absence of a phospholipid component within the heme pockets of these proteins (*29*).

Further considerations can be discussed by merging the results presented here with X-ray structural data obtained on HMP, FHP, and VHb to expand the current picture of the lipid-induced effects on the oxygen binding properties. The physical origin of the observed effects most likely resides in the steric hindrance of the acyl chain within the distal pocket that may impair free diffusion of diatomic ligands to the heme iron and favor ligand release. According to the highly conserved structure of the first shell of residues in contact with the iron-bound ligand in VHb, HMP, and FHP (Figure 7), it may be envisaged that the gaseous ligand entry is gated by the lipid chain (possibly the cyclopropyl moiety) in the phospholipid-bound protein which vicariates the LeuE11 isobutyl chain in the lipid-free protein. The gating effect of LeuE11 in VHb can be recognized in Figure 7 where the presence of the iron-bound azide ion entails the lateral diplacement of the isobutyl chain. Further work will be necessary to investigate the role of other distal pocket residues suggested to participate to the ligand stabilization in the lipid-free proteins, especially Tyr B10, which appears to be completely out of the iron ligand coordination sphere in the presence of the lipid in FHP (Figure 7).

## CONCLUSIONS

On the basis of the data presented here and the reports by Ollesch et al. (*26*) and Bonamore et al. (*15*), it may be hypothesized that lipid binding is a feature common to the whole flavohemoglobin and single-chain bacterial hemoglobin family; however, bacterial hemoglobins from different organisms might exhibit different specificities toward diverse phospholipid components. In fact, it should be stressed that many bacteria containing genes for "hemoglobin-like" proteins do not possess cyclopropanated fatty acids within the membrane (e.g., *Bacillus* species). In this framework, it would be of interest to determine whether these last bacterial hemoglobins are able to bind specific phosholipid components from the parent strain (e.g., methyl-branched phospholipids instead of cyclopropanated phospholipids in the *Bacillus* species). Thus, we also suggest that the nature of the bound lipid component can make substantial differences in the oxygen binding behavior and most likely affects other

oxygen-dependent catalytic properties of proteins such as NO dioxygenase (*30*, *31*) or alkylhydroperoxide reductase activity (*32*).

## REFERENCES


1. Frey, A. D., and Kallio, P. T. (2003) Bacterial hemoglobins and flavohemoglobins: Versatile proteins and their impact on microbiology and biotechnology, *FEMS Microbiol. Rev. 27*, 525−545.
2. Kallio, P. T., Tsai, P. S., and Bailey, J. E. (1996) Expression of *Vitreoscilla* hemoglobin is superior to horse heart myoglobin or yeast flavohemoglobin expression for enhancing *Escherichia coli* growth in a microaerobic bioreactor, *Biotechnol. Prog. 12*, 751−757.
3. Bhave, S. L., and Chattoo, B. B. (2003) Expression of *Vitreoscilla* hemoglobin improves growth and levels of extracellular enzyme in *Yarrowia lipolytica*, *Biotechnol. Bioeng. 84*, 658−666.
4. Geckil, H., Barak, Z., Chipman, D. M., Erenler, S. O., Webster, D. A., and Stark, B. C. (2004) Enhanced production of acetoin and butanediol in recombinant *Enterobacter aerogenes* carrying *Vitreoscilla* hemoglobin gene, *Bioprocess Biosyst. Eng. 26*, 325−330.
5. Kallio, P. T., and Bailey, J. E. (1996) Intracellular expression of *Vitreoscilla* hemoglobin (VHb) enhances total protein secretion and improves the production of α-amylase and neutral protease in *Bacillus subtilis*, *Biotechnol. Prog. 12*, 31−39.
6. Diez, B., Mellado, E., Fouces, R., Rodriguez, M., and Barredo, J. L. (1996) Recombinant *Acremonium chrysogenum* strains for the industrial production of cephalosporin, *Microbiologia 12*, 359−370.
7. Kim, Y., Webster, D. A., and Stark, B. C. (2005) Improvement of bioremediation by *Pseudomonas* and *Burkholderia* by mutants of the *Vitreoscilla* hemoglobin gene (vgb) integrated into their chromosomes, *J. Ind. Microbiol. Biotechnol. 32*, 148−154.
8. Khang, Y. H., Kim, I. W., Hah, Y. R., Hwangbo, J. H., and Kang, K. K. (2003) Fusion protein of *Vitreoscilla* hemoglobin with D-amino acid oxidase enhances activity and stability of biocatalyst in the bioconversion process of cephalosporin C, *Biotechnol. Bioeng. 82*, 480−488.
9. Chien, L. J., Wu, J. M., Kuan, I. C., and Lee, C. K. (2004) Coexpression of *Vitreoscilla* hemoglobin reduces the toxic effect of expression of D-amino acid oxidase in *E. coli*, *Biotechnol. Prog. 20*, 1359−1365.
10. Nilsson, M., Kallio, P. T., Bailey, J. E., Bulow, L., and Wahlund, K. G. (1999) Expression of *Vitreoscilla* hemoglobin in *Escherichia coli* enhances ribosome and tRNA levels: A flow field-flow fractionation study, *Biotechnol. Prog. 15*, 158−163.
11. Roos, V., Andersson, C. I., Arfvidsson, C., Wahlund, K. G., and Bulow, L. (2002) Expression of double *Vitreoscilla* hemoglobin enhances growth and alters ribosome and tRNA levels in *Escherichia coli*, *Biotechnol. Prog. 18*, 652−656.
12. Frey, A. D., and Kallio, P. T. (2005) Nitric oxide detoxification: A new era for bacterial globins in biotechnology? *Trends Biotechnol. 23*, 69−73.
13. Ramandeep, Hwang, K. W., Raje, M., Kim, K. J., Stark, B. C., Dikshit, K. L., and Webster, D. A. (2001) *Vitreoscilla* hemoglobin. Intracellular localization and binding to membranes, *J. Biol. Chem. 276*, 24781−24789.
14. Park, K. W., Kim, K. J., Howard, A. J., Stark, B. C., and Webster, D. A. (2002) *Vitreoscilla* hemoglobin binds to subunit I of cytochrome bo ubiquinol oxidases, *J. Biol. Chem. 277*, 33334−33337.
15. Bonamore, A., Farina, A., Gattoni, M., Schinina, M. E., Bellelli, A., and Boffi, A. (2003) Interaction with membrane lipids and heme ligand binding properties of *Escherichia coli* flavohemoglobin, *Biochemistry 42*, 5792−5801.
16. Ilari, A., Bonamore, A., Farina, A., Johnson, K. A., and Boffi, A. (2002) The X-ray structure of ferric *Escherichia coli* flavohemoglobin reveals an unexpected geometry of the distal heme pocket, *J. Biol. Chem. 277*, 23725−23732.
17. Tarricone, C., Galizzi, A., Coda, A., Ascenzi, P., and Bolognesi, M. (1997) Unusual structure of the oxygen-binding site in the dimeric bacterial hemoglobin from *Vitreoscilla*, *Structure 5*, 487−507.
18. Bolognesi, M., Boffi, A., Coletta, M., Mozzarelli, A., Pesce, A., Tarricone, C., and Ascenzi, P. (1999) Anticooperative ligand binding properties of recombinant ferric *Vitreoscilla* hemoglobin: A thermodynamic, kinetic and X-ray crystallographic structure, *J. Mol. Biol. 291*, 637−650.
19. Brockman, H. L. (1999) Lipid monolayers: Why use half a membrane to characterize protein-membrane interactions? *Curr. Opin. Struct. Biol. 9*, 438−443.
20. Maget-Dana, R. (1999) The monolayer technique: A potent tool for studying the interfacial properties of antimicrobial and membrane-lytic peptides and their interactions with lipid membranes, *Biochim. Biophys. Acta 1462*, 109−140.
21. Zhao, H. X., Rinaldi, A. C., Di Giulio, A., Simmaco, M., and Kinnunen, P. K. J. (2002) Interactions of the antimicrobial peptides temporins with model membranes. Comparison of Temporin B and Temporin L, *Biochemistry 41*, 4425−4436.
22. Giangiacomo, L., Mattu, M., Arcovito, A., Bellenchi, G., Bolognesi, M., Ascenzi, P., and Boffi, A. (2001) Monomer−dimer equilibrium and oxygen binding properties of ferrous *Vitreoscilla* hemoglobin, *Biochemistry 40*, 9311−9316.
23. Kundu, S., Premer, S. A., Hoy, J. A., Trent, J. T., III, and Hargrove, M. S. (2003) Direct measurement of equilibrium constants for high-affinity hemoglobins, *Biophys. J. 84*, 3931−3940.
24. Cherukuvada, S. L., Seshasayee, A. S., Raghunathan, K., Anishetty, S., and Pennathur, G. (2005) Evidence of a double-lid movement in *Pseudomonas aeruginosa* lipase: Insights from molecular dynamics simulations, *PLoS Comput. Biol.* (in press).
25. Ermler, U., Siddiqui, R. A., Cramm, R., and Friedrich, B. (1995) Crystal structure of the flavohemoglobin from *Alcaligees eutrophus* at 1.75 Å resolution, *EMBO J. 14*, 6067−6077.
26. Ollesch, G., Kaunzinger, A., Jucelka, D., Shubert-Zailavec, M., and Ermler, U. (1999) Phospholipid bound to the flavohemoprotein from *Alcaligenes eutrophus*, *Eur. J. Biochem. 262*, 396−405.
27. D'Angelo, P., Lucarelli, D., della Longa, S., Benfatto, M., Hazemann, J. L., Feis, A., Smulevich, G., Ilari, A., Bonamore, A., and Boffi, A. (2004) Unusual heme iron-lipid acyl chain coordination in *Escherichia coli* flavohemoglobin. *Biophys. J. 86*, 3882−3892.
28. Orii, Y., and Webster, D. A. (1986) Photodisociation of oxygenated cytochrome o (*Vitreoscilla*) and kinetic studies of reassociation, *J. Biol. Chem. 261*, 3544−3547.
29. Farres, J., Rechsteiner, M. P., Herold, S., Frey, A. D., and Kallio, P. T. (2005) Ligand binding properties of bacterial hemoglobins and flavohemoglobins, *Biochemistry 44*, 4125−4134.
30. Poole, R. K., Anjum, M. F., Membrillo-Hernandez, J., Kim, S. O., Hughes, M. N., and Stewart, V. (1996) Nitric oxide, nitrite, and Fnr regulation of hmp (flavohemoglobin) gene expression in *Escherichia coli* K-12, *J. Bacteriol. 178*, 5487−5492.
31. Gardner, P. R. (2005) Nitric oxide dioxygenase function and mechanism of flavohemoglobin, hemoglobin, myoglobin and their associated reductases, *J. Inorg. Biochem. 99*, 247−266.
32. Bonamore, A., Gentili, P., Ilari, A., Schinina, M. E., and Boffi, A. (2003) *Escherichia coli* flavohemoglobin is an efficient alkylhydroperoxide reductase, *J. Biol. Chem. 278*, 22272−22277.


BI052277N